Bioresource Technology 416 (2025) 131806

Contents lists available at ScienceDirect

Bioresource Technology

journal homepage: www.elsevier.com/locate/biortech

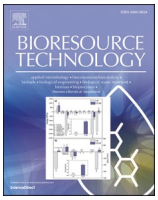

Engineering and evolution of *Yarrowia lipolytica* for producing lipids from lignocellulosic hydrolysates

Sangdo Yook [a,b,e], Anshu Deewan [a,c,e], Leah Ziolkowski [a,b], Stephan Lane [a,b,e], Payman Tohidifar [a,c,e], Ming-Hsun Cheng [a,d,e], Vijay Singh [a,d,e], Matthew J. Stasiewicz [b], Christopher V. Rao [a,c,e], Yong-Su Jin [a,b,e,*]

[a] *Carl Woese Institute for Genomic Biology, University of Illinois at Urbana-Champaign, Urbana, IL, USA*
[b] *Department of Food Science and Human Nutrition, University of Illinois at Urbana-Champaign, Urbana, IL, USA*
[c] *Department of Chemical and Biomolecular Engineering, University of Illinois at Urbana-Champaign, Urbana, IL, USA*
[d] *Department of Agricultural and Biological Engineering, University of Illinois at Urbana-Champaign, Urbana, IL, USA*
[e] *DOE Center for Advanced Bioenergy and Bioproducts Innovation, University of Illinois Urbana-Champaign, Urbana, IL, USA*

HIGHLIGHTS

- *Yarrowia lipolytica* was engineered and evolved for improved xylose assimilation.
- The resulting *Y. lipolytica* efficiently converted xylose into lipids.
- Genetic variations eliciting enhanced xylose assimilation were identified.
- Sorghum hydrolysate was efficiently converted into lipids by engineered *Y. lipolytica*.

GRAPHICAL ABSTRACT

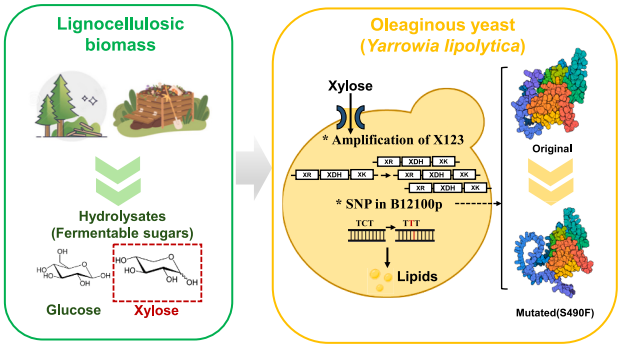

ARTICLE INFO

Keywords:
Yarrowia lipolytica
Adaptive laboratory evolution
Whole genome sequencing
Reverse engineering
Lignocellulosic hydrolysates

ABSTRACT

Yarrowia lipolytica, an oleaginous yeast, shows promise for industrial fermentation due to its robust acetyl-CoA flux and well-developed genetic engineering tools. However, its lack of an active xylose metabolism restricts the conversion of cellulosic sugars to valuable products. To address this, metabolic engineering, and adaptive laboratory evolution (ALE) were applied to the *Y. lipolytica* PO1f strain, resulting in an efficient xylose-assimilating strain (XEV). Whole-genome sequencing (WGS) of the XEV followed by reverse engineering revealed that the amplification of the heterologous oxidoreductase pathway and a mutation in the GTPase-activating protein gene (YALI0B12100g) might be the primary reasons for improved xylose assimilation in the XEV strain. When a sorghum hydrolysate was used, the XEV strain showed superior xylose consumption and lipid production compared to its parental strain (X123). This study advances our understanding of xylose metabolism in *Y. lipolytica* and proposes effective metabolic engineering strategies for optimizing lignocellulosic hydrolysates.

* Corresponding author.
E-mail address: ysjin@illinois.edu (Y.-S. Jin).

https://doi.org/10.1016/j.biortech.2024.131806
Received 27 May 2024; Received in revised form 9 September 2024; Accepted 10 November 2024
Available online 12 November 2024

1. Introduction

Yarrowia lipolytica, a member of the Hemiascomycetes family, is classified as a "non-conventional yeast" due to its unique properties that set it apart from a baker's yeast *Saccharomyces cerevisiae*. *Y. lipolytica* can utilize a diverse range of substrates, including n-alkanes, fats, and oils, and possesses various ABC transporters and *ex novo* pathways for substrate degradation (Beopoulos et al., 2011; Fukuda & Ohta, 2013). Notably, *Y. lipolytica* prefers respiratory metabolism over fermentative metabolism (Kavšček et al., 2015). Unlike a conventional yeast, *S. cerevisiae*, *Y. lipolytica* maintains a balanced metabolic flux from glucose to respiration (TCA cycle) without exhibiting a metabolic overflow phenotype, such as the production of ethanol through fermentation (Crabtree effect), resulting in high NADH and ATP yields (Crabtree, 1929; Malina et al., 2021). This unique metabolic flux distribution of *Y. lipolytica* makes it a promising producer of TCA cycle intermediates, such as succinic acid, α-ketoglutaric acid, and citric acid (Babaei et al., 2019; Guo et al., 2016; Yuzbasheva et al., 2019). *Y. lipolytica* is renowned for its significant lipid accumulation capacity, a trait that can be further enhanced through genetic engineering. As an oleaginous yeast, *Y. lipolytica* naturally accumulates more than 20 % of its cell biomass as lipids (Juanssilfero et al., 2018). Recent studies have shown that the lipid content of this yeast can be substantially increased by engineering pathways that enhance flux towards triacylglycerol (TAG) synthesis while simultaneously inhibiting peroxisome biogenesis and β-oxidation. Tai and Stephanopoulos (2013) overexpressed Acetyl-CoA carboxylase (ACC1) and diacylglycerol acyltransferase (DGA1) in the *Y. lipolytica* PO1g strain resulted in the production of 61.7 % intracellular lipids from glucose. Building on this work, the research group further enhanced NADPH supply by introducing NADP + -dependent glycerol-3-phosphate dehydrogenase (GPD) and malic enzyme pathways, alongside the implementation of the pyruvate/oxaloacetate/malate (POM) cycle and non-oxidative glycolysis (NOG) pathway (Qiao et al., 2017). This engineering strategy led to a lipid yield of 0.269 g lipid/g glucose, with an overall lipid content of 66.8 %. Another significant advancement was reported by a separate group, which successfully accumulated 90 % intracellular lipid content in the *Y. lipolytica* PO1f strain (Blazeck et al., 2014). This was achieved by overexpressing lipogenesis-related genes (such as DGA1) while simultaneously deleting genes involved in lipid oxidation (pex10, mfe1). Furthermore, in a non-W29 derived strain (NS18), overexpression of lipogenesis genes (DGA1, DGA2) coupled with the deletion of a lipase regulator (TGL3) resulted in a successful lipid production of 77 % (Friedlander et al., 2016). Additionally, *Y. lipolytica* can produce other acetyl-CoA-derived molecules, including carotenoids, and polyketides, making it an industrially important yeast (Cao et al., 2016; Lee et al., 2021; Spagnuolo et al., 2019; Tai & Stephanopoulos, 2013). With this potential to produce acetyl-CoA-derived value-added products, *Y. lipolytica* has been considered an industrially important yeast (Ledesma-Amaro & Nicaud, 2016).

Although *Y. lipolytica* has immense potential as an industrial workhorse microorganism, this yeast cannot metabolize xylose, the second most abundant sugar in nature, which hinders its strain development and utilization for producing cellulosic biofuels and chemicals (Jagtap & Rao, 2018; Prabhu et al., 2020). Microorganisms typically convert xylose to xylulose using two metabolic pathways. The first pathway involves two enzymes, D-xylose reductase (XR) and xylitol dehydrogenase (XDH), in yeast and mycelial fungi, with NADPH consumption by XR and NADH production by XDH, causing a cofactor imbalance. In contrast, the second pathway used by bacteria and anaerobic fungi involves a single enzymatic conversion by xylose isomerase (XI) without generating or consuming cofactors (NADH and NADPH) (Kwak & Jin, 2017). Xylulose is then further phosphorylated into xylulose-5-phosphate by xylulokinase (XK) and metabolized through the pentose phosphate pathway (PPP). *Y. lipolytica* possesses an endogenous xylose utilizing pathway, consisting of namely *ylXR* (YALI0D07634g), *ylXDH* (YALI0E12463g), and *ylXK* (YALI0F10923g) (Ryu & Trinh, 2021). However, the activities of these enzymes are not sufficient, limiting the efficient utilization of xylose by *Y. lipolytica* (Spagnuolo et al., 2018). To address this, previous studies engineered *Y. lipolytica* for efficient xylose assimilation. A heterologous oxidoreductase pathway from *Pichia stipitis* (*Ps*XR and *Ps*XDH) was introduced by Ledesma-Amaro et al. (2016) and Li and Alper (2016), resulting in the construction of engineered *Y. lipolytica* strains capable of utilizing xylose. Overexpression of the endogenous xylose assimilating enzymes in *Y. lipolytica* PO1f led to a 2.6-fold increase in xylose consumption (Rodriguez et al., 2016). Ryu and Trinh (2018) identified endogenous pentose sugar transporters (*TRP6*: YALI0C04730p, TRP22: YALI0B00396p) and observed positive effects on xylose utilization upon overexpression of these transporters in *Y. lipolytica*. Simultaneous overexpression of endogenous genes (*ylXR*, *ylXDH*, and *ylXK*) and phosphoketolase pathway-relevant genes (*XPKA* and *ACK* from *A.nidulans*) enabled efficient xylose assimilation in *Y. lipolytica* PO1d and facilitated cellulosic sugar utilization from lignocellulosic hydrolysates (Niehus et al., 2018). Yook et al. (2020) introduced a mutated xylose isomerase from *Piromyces* sp., resulting in an efficient lipid-producing *Y. lipolytica* strain without cofactor imbalance. However, these engineered *Y. lipolytica* strains for enhanced xylose assimilation still exhibited inefficient and slow xylose utilization. Moreover, while adaptive laboratory evolution (ALE) under xylose conditions identified mutations in evolved strains, the causality of the identified mutations for improving xylose assimilation has not been fully understood.

In this study, we aimed to improve xylose utilization in *Y. lipolytica* PO1f strain by overexpressing XR, XDH, and XK from *P. stipitis*, generating a xylose-utilizing *Y. lipolytica* (X123). Additionally, adaptive laboratory evolution (ALE) was employed to further enhance xylose assimilation, resulting in an evolved strain (XEV). To elucidate the relationship between identified genetic variations and the enhanced xylose assimilation phenotype in the XEV strain, we conducted whole-genome sequencing (WGS), enzyme assays, qPCR, and reverse engineering using a Cas9-based genome editing method. Finally, we evaluated the improved sugar utilization of the xylose-utilizing mutants by fermenting lignocellulosic hydrolysate obtained through the hydrothermal pretreatment of sorghum. This study provides genetic insights into xylose assimilation in *Y. lipolytica* and suggests potential metabolic engineering strategies for increasing the utilization of cellulosic sugars in lignocellulosic hydrolysates.

2. Materials and methods

2.1. Strains and Plasmids construction

Escherichia coli TOP10 (New England BioLabs, Ipswich, MA, USA) was used for general cloning and plasmid propagation. *E. coli* TOP10 cells were cultured in LB medium supplemented with 100 μg/mL ampicillin or appropriate antibiotics for selection at 250 rpm, 37 °C. The *Y. lipolytica* strain PO1f, a leucine and uracil auxotroph, was utilized as a parental yeast strain for engineering. The integrative plasmid pINT03 containing a selectable leucine marker was used to construct an expression cassette harboring oxidoreductase pathway genes, as previously described by Lane et al. (2015). Specifically, xylose metabolic pathway genes *XYL1*, *XYL2*, and *XYL3* from *P. stipitis* were codon-optimized for *Y. lipolytica* and introduced under the control of GPM1, TDH1, and FBA1 promoters, respectively into pINT03 through Gibson assembly, resulting in the plasmid pINT03-X123. The transformation of the *Y. lipolytica* PO1f strain with the pINT03 generated a control strain for a fair comparison, and the transformation of pINT03-XYL123 into the *Y. lipolytica* PO1f strain resulted in generating the X123 strain. The X123 strain was subjected to ALE based on serial sub-cultures in a xylose-containing YP medium (20 g/L of xylose, 20 g/L of peptone, and 10 g/L of yeast extract), resulting in the isolation of the XEV strain. The obtained engineered and evolved strain (X123 and XEV) and the control

strain were subsequently used for fermentation and whole-genome sequencing (WGS) analysis. The primer information used for plasmid construction is described in Table S1.

2.2. Media and culture conditions

To evaluate the ability of *Y. lipolytica* strains to utilize xylose, frozen yeast stocks were first inoculated into a rich medium (YPD) supplemented with 20 g/L of peptone, 20 g/L of glucose, and 10 g/L of yeast extract. The cells from the YPD culture were then transferred to 20 mL of YSC media containing either 20 g/L or 40 g/L of xylose, along with 0.79 g/L of a complete supplement mixture lacking leucine (CSM-Leu) and 1.7 g/L of Yeast Nitrogen Base (YNB) without amino acids and ammonium sulfate. To promote lipid accumulation, the C/N ratio was maintained at 100:1 using concentrated xylose and ammonium sulfate solution, resulting in a final concentration of 0.75 g/L of ammonium sulfate in the 40 g/L of xylose YSC medium.

To further assess the abilities of the parental and engineered strains to utilize a cellulosic hydrolysate, a sorghum hydrolysate was generated. The sorghum hydrolysate was prepared from a bioenergy sorghum bagasse that was subjected to hydrothermal pretreatment and disk milling, followed by enzymatic hydrolysis to release cellulosic sugars. The detailed preparation process of the sorghum hydrolysate is described in Cheng et al. (2019). The hydrolysate was then supplemented with ammonium sulfate at the final concentration of 0.82 g/L ammonium sulfate to provide nitrogen and filtered through a 0.2 μm filtration unit (Thermo Scientific) to prevent contamination and remove remaining solids. The filter-sterilized hydrolysate was frozen at −20 °C until use and then thawed at 4 °C for one day before fermentation. All fermentation steps were conducted in triplicate with constant agitation at 200 rpm and 28 °C.

2.3. Analytical methods

Cell density was quantified by measuring the optical density (OD600) at 600 nm using a UV–visible spectrophotometer (Biomate 5; Fisher, NY, USA). Dry cell weight (DCW) was determined by washing cells with deionized water three times and drying them overnight at 100 °C. High-performance liquid chromatography (HPLC) (Agilent, Santa Clara, CA, USA) with a Rezex ROA-Organic Acid H^+ (8 %) column (Phenomenex Inc.) was used to determine the concentrations of sugars (glucose and xylose) and other metabolites. The column and detector temperatures were kept at 50 °C, and a mobile phase of 0.005 M of sulfuric acid was used at a flow rate of 0.6 mL/min.

Total intracellular lipids were extracted using modified methods (Bligh & Dyer, 1959; Bourque & Titorenko, 2009; Yook et al., 2019). Briefly, 3–5 mL of culture broth containing yeast cells was collected, and the supernatant was removed by centrifugation. The remaining cells were stored at −20 °C for further analysis. Frozen cells were thawed at room temperature and mixed vigorously with an organic solvent mixture (chloroform and methanol, 2:1). The methanol phase was separated by adding the equivalent volume of water, and both chloroform and methanol phases were transferred to a new collection vial. Additional extraction was performed by adding 3 mL of chloroform to the remaining cells to ensure complete lipid extraction. The solvent mixture containing lipid extracts (chloroform phase) was separated from the water (methanol phase) through centrifugation at 3000 rpm for 15 min, and only the chloroform phase was transferred to a new vial. The chloroform phase containing total lipids was evaporated using a nitrogen evaporation system (Caliper Life Sciences, USA), and the lipid concentration and content were determined by calculating g lipid/mL sample and g lipid/g DCW, respectively.

2.4. Whole-genome sequencing analysis (WGS)

The Wizard® Genomic DNA Purification Kit (Promega) was used to extract total genomic DNA, followed by sequencing using an Illumina Novaseq with paired-end 150 cycles (2 x 150 bp) for each sample. The resulting number of reads per sample ranged from 43 to 53 million. Before mapping to the reference genome, sequencing adapters and primer sequences were removed using the Trimmomatic toolkit (version 0.38). To analyze the genome sequencing data of the mutant strains, we adapted the GATK best practices workflow for a yeast genome (Van and O'connor, 2020). This workflow involved using the "Data pre-processing for variant discovery" and "Germline short variant discovery (SNPs + Indels)" workflows from GATK, which can be found at https://gatk.broadinstitute.org/hc/en-us/sections/360007226651-Best-Practices-Workflows. The *Y. lipolytica* PO1f reference genome (GeneBank accession number: GCA_009372015.1) was indexed, and short-reads were mapped using Burrows-Wheeler Aligner (BWA version 0.7.17) (Li & Durbin, 2009). The alignment files were pre-processed for variant calling using GATK version 4.1.4.0 (McKenna et al., 2010) and SAMtools version 1.11 (Li et al., 2009) according to the guidelines from the GATK workflow. HaplotypeCaller in Genome Analysis Tool Kit (GATK) was used for variant calling, followed by the VariantFiltration tool (GATK version 4.1.4.0). Read coverage and read-depth were calculated using SAMtools version 1.11 and CNVKit version 0.9.8, respectively. Finally, all vcf files were functionally annotated using R packages, including GenomicRanges, Biostrings, Rsamtools, VariantAnnotation, and snpStats. The ggplot2 and ggpubr R packages were used for plotting and data visualization. The scripts used in this analysis are available at github.com/raogroupuiuc/yl_variantcalling.

2.5. Enzyme activity assays

The enzyme activities of XR and XDH were measured using an assay based on the protocol described by Lee et al. (2012). To prepare the crude enzyme, 1 mL of *Y. lipolytica* cells were grown in a YPD medium and harvested through centrifugation at 6000 rpm at room temperature. After resuspending the pellet using 50 mM phosphate buffer (pH 7.0), cell disruption was performed using a bead beater (Fastprep-24, MP Bio) with three cycles of vortexing with 0.2g beads, each followed by 4 min cooling. After centrifugation at 4 °C and 15,000 rpm, the supernatant containing crude enzyme was used for the assay. For the XR assay, a mixture of 0.4 mM NADPH, 50 mM potassium phosphate buffer (pH 6.0), and 200 mM xylose was combined with the extracted crude enzyme. For XDH, 50 mM Tris-HCl buffer (pH 8.5), 300 mM xylitol, 50 mM $MgCl_2$, and 2 mM NAD^+ were mixed with crude enzyme. All reagents were freshly prepared and mixed immediately before the reaction. The conversion of NADPH and NAD^+ was confirmed by measuring the absorbance at 340 nm with a 96-well plate reader (BioTek, USA). Enzyme activity was defined as the amount of oxidized 1 μmol NADPH or reduced NAD^+ per minute per milligram of protein, with 1 unit representing the activity of 1 μmol NADPH or NAD + per minute. All experiments were performed in triplicate.

2.6. Measurement of expression levels (qPCR)

The cells of xylose-utilizing mutants and control strain were grown up to an exponential phase, and RNA extraction was conducted to measure the expression level of endogenous xylose metabolizing enzymes (*ylXR*: YALI0D07634g, *ylXDH*: YALI0E12463g, and *ylXK*: YALI0F10923g) and heterologous oxidoreductase pathway (*PsXYL1*, *PsXYL2*, and *PsXYL3*) genes in each strain. Briefly, cells were grown overnight in a YPD medium and re-inoculated in a YPX medium containing 20 g/L of xylose to enrich the mRNA expression in the cells. After growing cells for an additional day, RNA was extracted using an RNeasy plus mini kit (Qiagen). Immediately after RNA extraction, cDNA was synthesized using 500 ng of total RNA and the SuperScript cDNA synthesis kit (Invitrogen). Before qPCR, primer efficiency calculation was conducted to evaluate the priming efficiency, and primers only showing an efficiency between 90–110 % were used for the further qPCR step.

Regarding qPCR analysis, 1.5 μL of synthesized cDNA was mixed with SYBR Green Master Mix (Bio-rad), and each reaction was performed in 96-well plates using T100™ Thermal Cycler (Bio-rad). All reactions were conducted in biological triplicate, and the fold changes were calculated through the $2^{-\Delta\Delta CT}$ methods and normalized with the *ACT1* gene (Rao et al., 2013).

2.7. Reverse engineering of identified mutations

Three potential genes (YALIB012100g, YALIB018282g, and YALI0E18117g) identified as responsible genes for eliciting the improved xylose assimilation of the XEV strain were selected through whole genome sequencing (WGS) analysis. Reverse engineering studies based on their function and the impact of mutations were performed by introducing point mutations found in the XEV strain into the X123 strain using Cas9-based genome editing. Specifically, crRNAs were designed to induce double-strand breaks in the target regions of Cas9 using the online tool https://chopchop.cbu.uib.no (Labun et al., 2019). The top three crRNA candidates with the highest scores were fused with trRNA and cloned into the JME4599 vector (Addgene #129660). Linear donor DNA containing the desired mutations with 50 bp homology arms of target loci was generated by overlap extension PCR. The sgRNA sequence information and primer details used for overlap extension PCR are presented in Table S2. The transformation of both linear donor DNA and sgRNA was carried out using the LiAc method described in Jagtap et al. (2021); Markham et al. (2018). Following transformation, the cells were incubated in YPD medium for 3 h and then plated onto YSC-Leu-clonNAT medium containing 20 g/L glucose, 0.79 g/L complete supplement mixture (CSM-Leu), 1.7 g/L Yeast Nitrogen Base (YNB), and 100 μg/ml nourseothricin (clonNAT). Colonies were isolated after 2–4 days of incubation, and the targeted loci were amplified via PCR amplification after extracting genomic DNA from each sample. Sanger sequencing was performed on 10 samples from each genome-editing, and only verified colonies were used for further phenotype validation.

3. Results and Discussion

3.1. Introduction of the heterologous oxidoreductase pathway and ALE

To enhance xylose assimilation in *Y. lipolytica*, the xylose-utilizing *Y. lipolytica* X123 was constructed by introducing the oxidoreductase pathway from *Pichia stipitis* into the *Y. lipolytica* PO1f strain. To further improve the xylose assimilation capacity, the X123 strain underwent an adaptive laboratory evolution (ALE) process under xylose conditions. During the 450-hour ALE process, the PO1f strain showed negligible xylose consumption, while the X123 strain exhibited a gradual improvement in xylose consumption, completely depleting 40 g/L of xylose within 112 h after the 4th round of serial sub-culture (Figure S1). Following six rounds of serial sub-cultures, individual colonies were isolated and subjected to a xylose consumption test. The most efficient xylose-metabolizing strain, XEV, was selected for further studies.

Additionally, to assess the successful introduction of the oxidoreductase pathway and the subsequent changes in redox balance after ALE, intracellular NAD+/NADH and NADP+/NADPH ratios were measured. When glucose was used as the carbon source, no significant differences were observed in the NAD+/NADH and NADP+/NADPH ratios among the PO1f, X123, and XEV strains (Figure S2). However, when xylose was used as the carbon source, both the X123 and XEV strains exhibited significantly lower NAD+/NADH ratios and higher NADP+/NADPH ratios compared to their levels during glucose fermentation. These results indicate that while the oxidoreductase pathway was successfully introduced, cofactor imbalance during xylose utilization persists in the engineered *Y. lipolytica* strains, even after ALE.

To validate the xylose assimilating and lipid producing capacities of engineered *Y. lipolytica* strains, xylose fermentation was carried out in a nitrogen-controlled minimal medium (YSC) with 40 g/L of xylose as a sole carbon source. *Y. lipolytica* lacks active xylose assimilating enzymes. Therefore, a parental strain (PO1f) was unable to grow in a xylose medium (Fig. 1a-b). However, with the introduction of a heterologous oxidoreductase pathway, the X123 strain was able to grow on xylose, and the cell density reached OD600 = 10.6 at 160 hrs after consuming a half (20 g/L of xylose) of provided xylose. The XEV strain, which was obtained through ALE of the X123 strain, showed drastically enhanced growth and xylose utilization, resulting in the highest cell density of OD600 = 14.1 at 112 hrs, after complete consumption of 40 g/L of xylose. However, at a higher xylose concentration (100 g/L), the XEV strain exhibited limited xylose consumption, utilizing only 50 g/L within 140 h in a minimal medium (Figure S3a). In contrast, in a parallel experiment using a rich medium (YPX), the XEV strain completely consumed 80 g/L of xylose within 100 h (Figure S3b). This discrepancy is likely due to the limited availability of nutrients and growth factors in the minimal medium. However, the high nitrogen content in the rich medium is not conducive to controlling the C/N ratio necessary for optimal lipid accumulation. Therefore, in this study, the YSC minimal medium was used with the C/N ratio adjusted to 100 to induce lipid synthesis in the strains. When the total lipid contents and titer of the PO1f, X123, and XEV strains were measured, the XEV strain exhibited the highest lipid concentration and content, 2.47 g lipid/L and 34.92 % (g lipid/g cell*100), respectively, at 90 hrs (Fig. 1c). The X123 strain accumulated only 0.4 g lipid/L and 25 % (g lipid/g cell*100) at 90 hrs. Notably, this result aligns with previous findings where strains with the introduced oxidoreductase pathway synthesized over 20 % intracellular lipids under nitrogen-limited conditions (Rodriguez et al., 2016; Niehus et al., 2018). Although the PO1f strain did show minimal lipid accumulation, as shown in Fig. 1c, this accumulation was negligible compared to the significant lipid production observed in the X123 and XEV strains during the fermentation process. A comparative analysis of the specific growth rates, xylose consumption rates and lipid content of previously developed xylose-utilizing strains is presented in Table 1.

These results suggest that some genetic variations accumulated in the XEV strain during ALE might have improved the innate xylose metabolism toward lipid accumulation. Therefore, we conducted WGS to identify genetic variations related to xylose metabolism in the XEV strain.

3.2. Amplification of the heterologous oxidoreductase pathway genes in the XEV

As the reference genome of the *Y. lipolytica* PO1f is publicly available, whole-genome-sequenced DNA fragments of the XEV strain were aligned to the PO1f reference genome. Genetic variants were identified by comparing the reference genome sequence and aligned DNA fragments.

In addition, to identify the integration site of the heterologous oxidoreductase pathway, de novo assembly was performed using SPAdes (Baker, 2012; Pendleton et al., 2015). Whole-genome sequencing data were utilized to assemble raw reads into scaffolds with SPAdes (ver. 3.15.5). These scaffolds were then analyzed to locate sequences flanking the oxidoreductase pathway, thereby determining its integration site. Specifically, the genome of the X123 strain was assembled, and a local BLAST+ (ver. 2.13.0) database was created from the scaffolds to compare against the oxidoreductase pathway sequence. The analysis revealed that the oxidoreductase pathway was integrated 37 bp downstream of the YALI0C00385g gene, which encodes a hypothetical protein (Figure S4). However, due to the nature of hypothetical proteins, the impact on xylose metabolism is likely minimal.

Through read depth analysis, we found that the genome of the XEV strain showed 6.75 to 7.22 times higher read depth of the introduced expression cassette than that of the X123 strain (Table 2), suggesting that the heterologous oxidoreductase pathway genes were amplified during ALE. Gene amplification is a well-documented phenomenon in both natural evolution and ALE, where selective pressure can lead to the

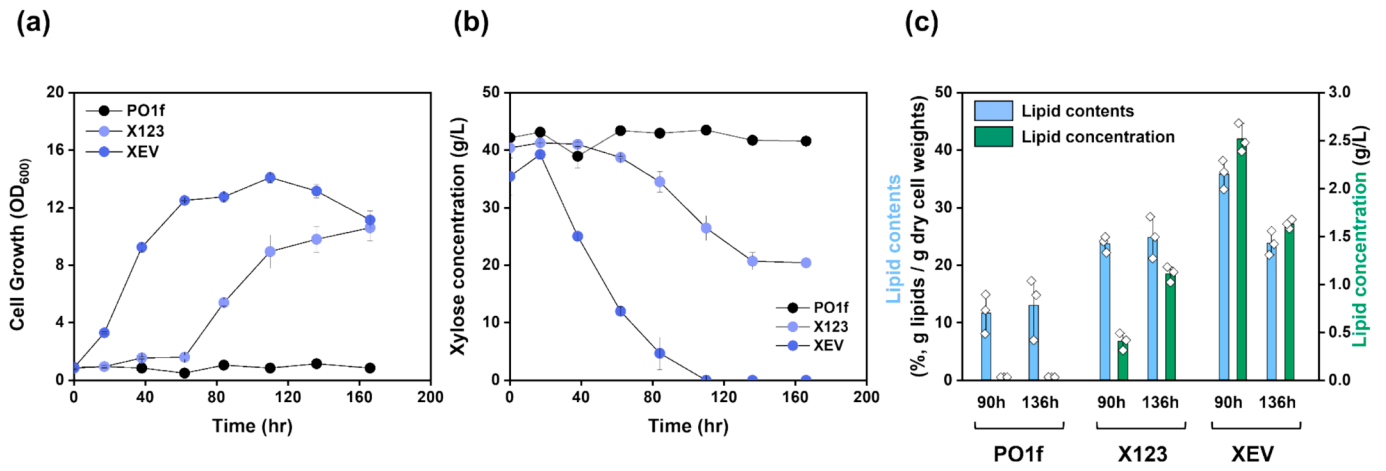

Fig. 1. Fermentation profiles of xylose-utilizing *Y. lipolytica* mutants (X123 and XEV) and control (PO1f) strain; (a) Cell growth, (b) Xylose consumption, (c) Lipid concentrations and contents. The experiments were conducted in biological triplicate.

Table 1
Comparison of xylose fermentation and lipid producing capacity under flask fermentation.

Organism	Strain	Genotype	Specific growth rate (μ)	Xylose consumption rate (g/L/h)	Lipid content (%)	Reference
Y. lipolytica	PO1f:XDH + XKS	PO1f ylXDH ylXK	0.032	0.128	21	Rodriguez et al. (2016)
	E26 XUS	E26 ssXR ssXDH	0.057	0.25	NA	(Li and Alper (2016))
	XYL+	PO1d ssXR ssXDH ylXK	0.065	0.42	17 (Fatty acid in DCW)	Ledesma-Amaro et al. (2016)
	YSX	PO1f Xyl3A* ylXK	0.017	0.16	30.16	Yook et al. (2020)
	XEV	PO1f ssXR ssXDH ssXK	0.051	0.35	34.92	This study

Table 2
Read depth and copy number variation in the X123 and XEV strains before and after ALE. Significant differences in read depths of the heterologous genes coding for XR, XDH, and XK were observed between the two strains.

Median values	Read Depth		Copy Number
Genes	X123	XEV	XEV / X123
XR	789	5699	7.22
XDH	869	5870	6.78
XK	835	5716	6.83

increased copy number of advantageous genes, providing a competitive growth advantage under specific conditions (Demeke et al., 2015; dos Santos et al., 2016; Oh et al., 2016). In our study, the selective pressure during ALE was designed to enhance xylose assimilation, which likely drove the amplification of genes in the oxidoreductase pathway. The increased gene copy number likely resulted in higher expression levels of key enzymes, such as XR, XDH and XK which are crucial for efficient xylose metabolism.

To confirm our hypothesis that heterologous oxidoreductase pathway genes were amplified, we measured the activities of the XR and XDH by extracting crude enzymes from xylose-utilizing mutants (X123 and XEV) and the control strain (PO1f). The results showed that the XR and XDH activities of the XEV strain were 5.64 and 3.36 times higher than those of the X123 strain, respectively (Fig. 2a). However, it is premature to conclude that these enhanced enzyme activities resulted from the amplification of heterologous genes because *Y. lipolytica* harbors endogenous oxidoreductase pathway genes (*ylXR*: YALI0D07634g,

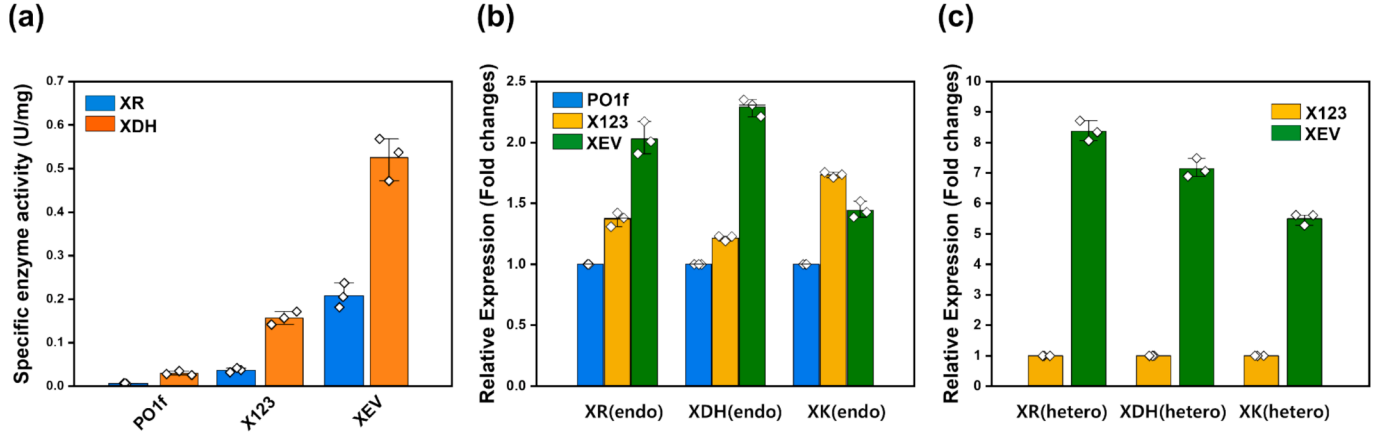

Fig. 2. Confirmation of genetic variations identified through WGS; (a) Enzymatic assays of XR and XDH, (b) qPCR analysis of endogenous genes (ylXR: YALI0D07634g, ylXDH: YALI0E12463g, and ylXK: YALI0F10923g), and (c) qPCR analysis of heterologous genes coding for XR, XDH, and XK.

ylXDH:YALI0E12463g, and *ylXK*:YALI0F10923g), although the activities of these genes are not active. During ALE, the expression of the corresponding endogenous genes may have increased but the heterologous ones were not. To address this speculation, we compared gene expression levels through qPCR to determine whether the enhanced enzyme activities were derived from endogenous or heterologous genes (Fig. 2b-c). The results showed that the expression levels of endogenous genes increased slightly after ALE, but the fold changes were marginal (1.2–2.4 times) as compared to those of heterologous genes (5.2–8.3 times). This finding suggests that the amplified heterologous oxidoreductase pathway genes, not endogenous ones, might be a primary reason for enhanced xylose assimilation in the XEV strain.

3.3. Identification of unique genetic variations in the XEV strain and reverse engineering for validation

Understanding how *Y. lipolytica* reprograms its genetic network to ferment xylose during the adaptive laboratory evolution (ALE) process is crucial. Therefore, to gain insight into the genetic variations relevant to xylose assimilation in *Y. lipolytica*, whole-genome sequencing analysis was conducted by comparing the genome sequences of strains and the reference genome. The comparison of the analyzed genome sequences of the XEV strain with the strains before ALE (PO1f and X123) identified eight genetic variations in open reading frame (ORF) unique to the XEV strain, as shown in Table 3. Based on their functions and the consequences of mutations, BKA90DRAFT_137339 (YALI0B12100p) coding for GTPase-activating protein, BKA90DRAFT_109120 (YALI0E18117p) coding for E3 ubiquitin-protein ligase, and BKA90DRAFT_141891 (YALI0B18282p) coding for cAMP-independent were selected for the validation through reverse engineering. Previous studies have demonstrated that the nonsense mutation of *IRA2* coding for GTPase-activating protein in *S. cerevisiae* increased xylose utilization and ethanol production (Sato et al., 2016; Tanaka et al., 1991). Additionally, Nijland et al. (2016); Papapetridis et al. (2018) reported that the deletion of *RSP5* E3 ubiquitin-protein ligase prevented ubiquitination of hexose transporters and increased xylose uptake rate in *S. cerevisiae*.

While genetic variations in promoters or terminators could have influenced the expression levels of the heterologous oxidoreductase pathway genes, as shown in Table S3, this study primarily focused on reverse engineering the mutations found within protein-coding ORFs. This focus is due to the higher likelihood of these variations directly impacting xylose metabolism (Breunig et al., 2014).

To determine the contributions of the selected mutations toward enhanced xylose assimilation in the XEV strain, targeted deletions of three selected proteins were made in the XEV strain using Cas9-based genome editing (Figure S5). Deletion of YALI0E18117g, encoding the E3 ubiquitin-protein ligase, proved difficult to get the mutant due to its essential role in posttranslational modification processes (Zheng & Shabek, 2017). Therefore, fermentation experiments were conducted using the YALI0B12100g and YALI0B18282g deleted strains, as no significant differences in cell growth or xylose consumption were observed compared to the XEV strain (Figure S5b-d). Additional reverse engineering was performed by introducing three mutations into the non-evolved strain (X123) one by one using CRISPR-Cas9, creating three different mutants (Figure S6a). Sanger sequencing was performed to verify that the mutations were properly introduced (Figure S6b). The mutations at YALI0E18117p (D462N) and YALI0B18282p (Q364*) (XEVmt2 and XEVmt3 strains) did not result in significant differences in cell growth or xylose assimilation compared to the control strain (X123) (Fig. 3). However, the mutation at YALI0B12100p (S409F) (XEVmt1 strain) led to significant differences in cell growth and xylose assimilation, indicating that the single-nucleotide polymorphism (SNP) in YALI0B12100p (S409F) might be responsible for xylose assimilation in *Y. lipolytica*. To investigate possible synergistic effects on xylose assimilation among the selected SNPs, the mutations in YALI0B12100p and YALI0B18282p were introduced simultaneously in the X123 strain. The strain with mutation in YALI0E18117p was excluded from this experiment as it was not associated with xylose assimilation in *Y. lipolytica*, evidenced by the absence of changes in xylose assimilation when the SNP was introduced in the X123 strain (Fig. 3). The strain with dual SNPs at YALI0B12100p and YALI0B18282p showed a slight increase in growth and xylose consumption rate compared to the XEVmt1 strain. However, there was no statistical significance.

Taken together, the mutation (S409F) in YALI0B12100, which encodes a GTPase-activating protein, was identified as being associated with the enhanced xylose-assimilating phenotype observed in the XEV strain. This mutation likely causes a loss of function in the GTPase-activating protein. In normal cells, GTP-bound Ras1 and Ras2 proteins increase intracellular cAMP levels, which, in turn, activate PKA (Protein Kinase A) signaling pathways. These pathways then enhance the activities of various transcription factors involved in processes such as glycolysis, trehalose biosynthesis, stress responses, and ribosomal protein expression (Conrad et al., 2014).

In the XEV strain, the S409F mutation likely reduces the GTPase activity, leading to a decrease in the conversion of GTP-bound Ras proteins to their inactive GDP-bound form. This reduction in GTPase activity could result in sustained or elevated levels of cAMP, thereby hyperactivating the cAMP-PKA signaling pathway. The hyperactivation of this pathway may contribute to the observed increase in xylose assimilation by enhancing the expression or activity of key enzymes involved in xylose metabolism.

Structural analysis using Alphafold2 (Jumper et al., 2021) supports this hypothesis, indicating that the S409F mutation leads to significant alterations in the GTPase-activating protein's structure, likely resulting in the complete loss of its original function (Figure S7). This connection between the GTPase-activating protein mutation and enhanced xylose

Table 3
Genetic variations that are uniquely existing in the XEV strain. Based on the function of proteins and the consequences of mutation, three candidates (YALI0B12100p, YALI0E18117p, and YALI0B18282p) were selected for further reverse engineering.

Gene ID	Nucleotide Change	Amino acid Change	Function of protein
BKA90DRAFT_137339	C → T	D165D	Cytochrome P450 52A12 (YALI0E23474p)
BKA90DRAFT_133446	T → TTGTGTGTGTGTGTGTGTGTGTGTGTGTGTGTGTGTGTGTGTGTGTG	frameshift	Cutinase gene palindrome-binding protein (YALI0F05346p)
BKA90DRAFT_117863	G → A	S409F	GTPase-activating protein (YALI0B12100p)
BKA90DRAFT_156218	A → ACATCAGCTGTAGTTGTAACAGAAGTAGCAGCTGAAGTAGATG	V252ASTSAATSVTTTADV	Cell surface glycoprotein (YALIE18700p)
BKA90DRAFT_43958	TTTTTTTTTTTTTTTTTTTTTTTTTTTTTTTTTTA → T	frameshift	Hypothetical protein
BKA90DRAFT_109120	G → A	D462N	E3 ubiquitin-protein ligase RSP5 (YALI0E18117p)
BKA90DRAFT_35865	GC → G	frameshift	FYVE domain containing protein (YALI0F32065p)
BKA90DRAFT_141891	C → T	Q364*	cAMP-independent regulator protein (YALI0B18282p)

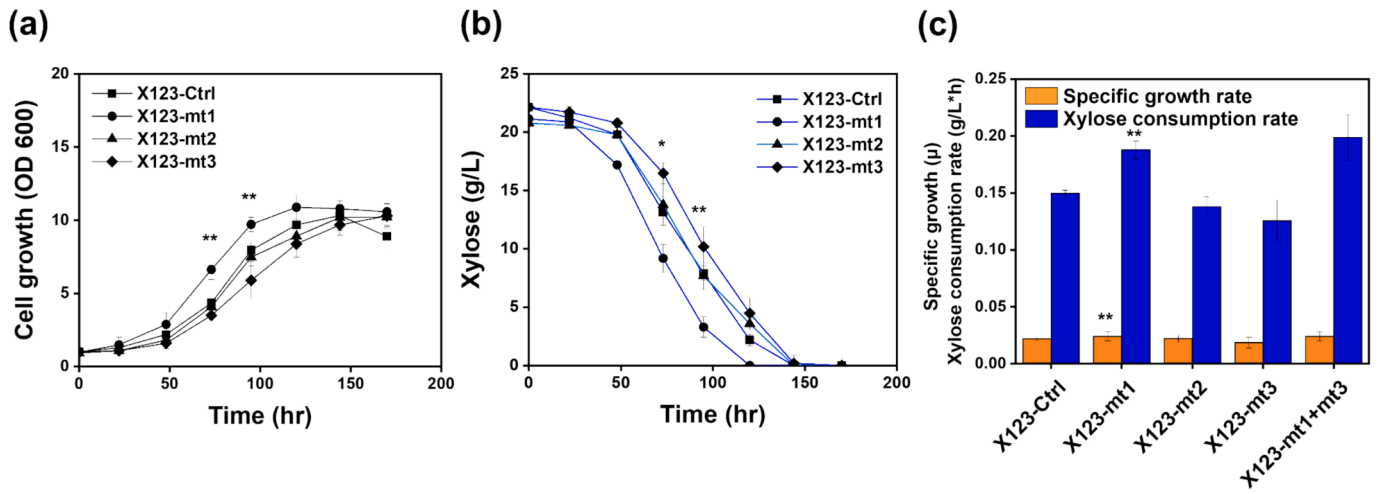

Fig. 3. Fermentation profiles of reverse-engineered mutants; (a) Cell growth, (b) Xylose consumption, (c) Specific growth rate, and xylose consumption rates. The student's *t*-test was conducted to describe statistical differences between mutants and control. Only the X123-mt1 strain (YALI0B12100p reversely engineered, S409F) showed a significant difference compared to the control. **p < 0.01 vs control, *p < 0.05 vs control.

metabolism has also been observed in *Saccharomyces cerevisiae*, where similar mutations have been linked to improved xylose utilization (Sato et al., 2016).

In conclusion, while the S409F mutation in YALI0B12100p is a key factor influencing xylose metabolism in the XEV strain, the primary driver of the enhanced xylose assimilation is the amplification of the oxidoreductase pathway genes (Fig. 4). Therefore, the most effective strategy for constructing an efficient xylose-utilizing *Y. lipolytica* strain is to combine the strong expression of the oxidoreductase pathway with the introduction of the YALI0B12100p S409F mutation using CRISPR-Cas9.

3.4. Lipid production using a lignocellulosic hydrolysate

We performed fermentation experiments using a sorghum hydrolysate to compare the sugar consumption and lipid synthesis abilities of the PO1f, X123 and XEV strains (Fig. 5). The hydrolysate, prepared through hydrothermal treatment of sorghum bagasse, contained 19.8 g/L of glucose and 9.5 g/L of xylose, which are lower than those in other lignocellulosic hydrolysates treated with strong acids or bases (Fig. 5a). The concentration of fermentation of inhibitors in the sorghum hydrolysate used in this study is presented in Table S6. Both the X123 and XEV strains consumed xylose in the hydrolysate faster than its parental strain (PO1f) after glucose consumption was completed within 48 h (Fig. 5b-d). During the fermentation period of 24–46 h, while glucose remained unutilized, the X123 and XEV strains simultaneously consumed 3.9 g/L and 5.1 g/L of xylose, respectively. This indicates that the carbon catabolite repression (CCR) effect in *Y. lipolytica* is milder compared to other strains that strongly favor glucose. Ryu et al. (2015) suggested that the milder CCR observed during glucose and xylose co-fermentation in *Y. lipolytica* is due to its wide range of sugar transporters and the weak transcriptional repression of xylose metabolic enzymes and transporters. Interestingly, despite the presence of 20 g/L of glucose in the sorghum hydrolysate, the PO1f strain was unable to consume all the glucose by the end of fermentation. This is likely due to the inhibitory effects of acetate present in the hydrolysate. While *Y. lipolytica* is known to be more tolerant to acetate than other yeasts (Koh et al., 2024), co-fermentation with glucose, as opposed to xylose, significantly inhibits growth at similar concentrations (Konzock et al., 2021). Moreover, recent studies on xylose and acetate co-fermentation in yeast have

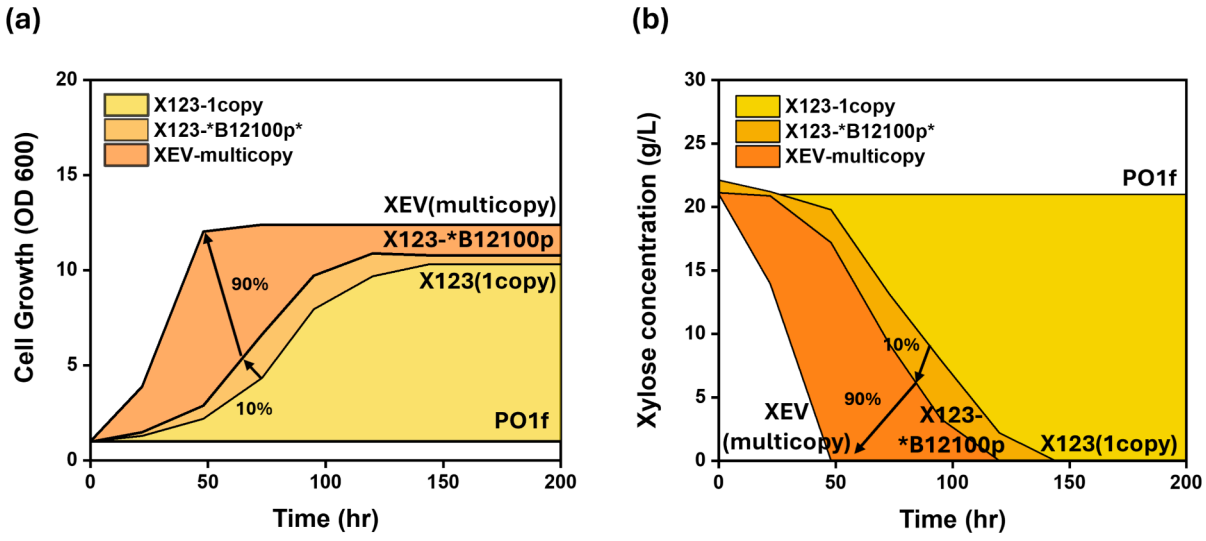

Fig. 4. Illustration of contributions of amplified XR, XDH, and XK and the point mutation (S409F) in GTPase-activating protein (YALI0B12100p, S409F) toward the enhanced xylose assimilation capacity of the XEV strain; 90% of the xylose-consuming capacity of XEV strain comes from amplified oxidoreductase pathway genes and remaining 10% comes from the mutation (S409F).

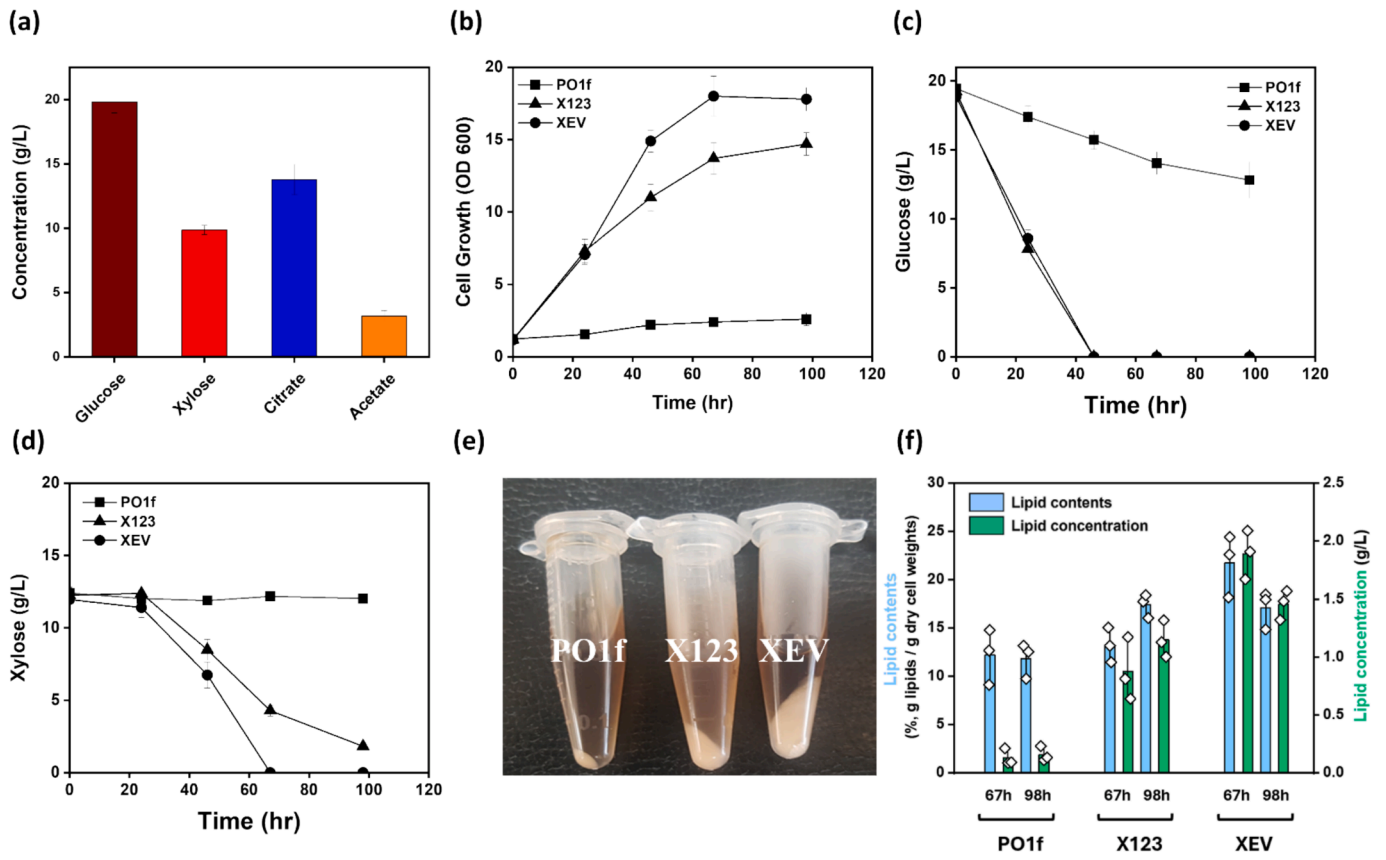

Fig. 5. Fermentation of xylose-utilizing *Y. lipolytica* mutants using sorghum hydrolysate; (a) Composition of the sorghum hydrolysate, (b) Cell growth (OD600), (c) Glucose consumption, (d) Xylose consumption, (e) Comparison of biomass after the fermentation, (f) Lipid concentration and contents at 67 and 98 h.

shown that acetate, which acts as an inhibitor in glucose fermentation, can serve as an excellent source of acetyl-CoA during xylose fermentation (Sun et al., 2021). In our study, the X123 and XEV strains, which possess xylose-assimilating capabilities, are likely to detoxify acetate during fermentation, whereas the PO1f strain, which cannot metabolize xylose, experiences inhibition by acetate, impairing glucose metabolism. Additionally, the high citrate concentration present in the sorghum hydrolysate could also be acting as an inhibitor during glucose fermentation. Further studies are needed to understand the interactions between citrate and lignocellulosic sugars during co-fermentation in *Y. lipolytica*.

The metabolic pathway for converting glucose and xylose from lignocellulosic hydrolysate to lipids in *Y. lipolytica* involves the initial catabolism of these sugars via glycolysis and the pentose phosphate pathway, respectively. Glucose is primarily converted to acetyl-CoA through glycolysis, while xylose, after being converted to xylulose-5-phosphate, feeds into the pentose phosphate pathway and eventually glycolysis. Acetyl-CoA, a key precursor in lipid biosynthesis, enters the lipid production pathway where it is converted into fatty acids through fatty acid synthase (FAS). These fatty acids are subsequently esterified to form triacylglycerols (TAGs), which accumulate as intracellular lipids. The metabolic pathway for lipid synthesis from glucose and xylose is detailed in Figure S8.

Due to the amplification of heterologous oxidoreductase pathway genes and the mutation in the GTPase activating protein (YALI0B12100p), the XEV strain had superior xylose assimilation capacity and consumed all the xylose present in the hydrolysate, whereas the X123 strain could not deplete all the sugars during the entire fermentation. The XEV strain's enhanced xylose assimilating capacity impacted biomass and lipid accumulation, resulting in the highest cell growth and lipid content (Fig. 5e-f). It is noteworthy that the XEV strain exhibited identical glucose consumption compared to the X123 strain during hydrolysate fermentation, despite initially displaying impaired cell growth and glucose consumption when glucose was the sole carbon source (Figure S9). This phenomenon could be attributed to the deletion of the threonine aldolase gene. A read-depth analysis of the entire *Y. lipolytica* genome revealed a significantly lower XEV/X123 ratio for a specific scaffold (ML756117.1), suggesting that this scaffold may have been entirely deleted during the ALE process (Table S4). One of the proteins encoded by this scaffold is threonine aldolase (YALI0A21417p), which catalyzes the cleavage of threonine into glycine and acetaldehyde, both of which are intermediates in central metabolic pathways (Table S5). Specifically, this deletion could impair glycine metabolism, which is responsible for generating NADH, thus reducing NADH production. During glucose fermentation, insufficient NADH production could limit fermentation efficiency. However, during co-fermentation with xylose, where excess NADH is produced by the XDH gene, this limitation is alleviated. Consequently, the XEV strain appears to be optimally suited for hydrolysate fermentation containing both glucose and xylose. In conclusion, we successfully constructed an efficient sugar-utilizing *Y. lipolytica* strain through the combined application of metabolic engineering and ALE. This study's significance lies in broadening the genetic understanding of xylose metabolism in *Y. lipolytica*, which could be applied to further strain development of *Y. lipolytica* for the production of biofuels and chemicals from lignocellulosic hydrolysates.

4. Conclusion

We identified necessary genetic perturbations to enhance xylose metabolism in *Y. lipolytica* through metabolic engineering and adaptive laboratory evolution (ALE). WGS, RT-PCR, and enzymatic analysis of the rapid xylose assimilating strain (XEV) revealed that high activities of XR,

XDH, and XK are essential and a point mutation in gene YALI0B12100g can further xylose assimilation. Using lignocellulosic hydrolysate, our engineered and evolved strain (XEV) produced lipids at 2.3 times the rate of the control, improving from 0.83 g/L to 1.94 g/L. These results advance our understanding of xylose metabolism in *Y. lipolytica*, and its industrial application for converting cellulosic sugars to value-added products.

CRediT authorship contribution statement

Sangdo Yook: Writing – original draft, Visualization, Methodology, Investigation, Formal analysis. **Anshu Deewan:** Writing – original draft, Methodology, Investigation, Formal analysis. **Leah Ziolkowski:** Methodology, Investigation. **Stephan Lane:** Methodology, Investigation. **Payman Tohidifar:** Methodology. **Ming-Hsun Cheng:** Methodology. **Vijay Singh:** Methodology. **Matthew J. Stasiewicz:** Writing – review & editing. **Christopher V. Rao:** Writing – review & editing, Supervision. **Yong-Su Jin:** Writing – review & editing, Supervision, Funding acquisition, Conceptualization.

Declaration of competing interest

The authors declare that they have no known competing financial interests or personal relationships that could have appeared to influence the work reported in this paper.

Acknowledgments

This work was funded by the DOE Center for Advanced Bioenergy and Bioproducts Innovation (U.S. Department of Energy, Office of Science, Biological and Environmental Research Program under Award Number DE-SC0018420). Any opinions, findings, and conclusions or recommendations expressed in this publication are those of the author (s) and do not necessarily reflect the views of the U.S. Department of Energy.

Appendix A. Supplementary data

Supplementary data to this article can be found online at https://doi.org/10.1016/j.biortech.2024.131806.

Data availability

Data will be made available on request.

References

Babaei, M., Rueksomtawin Kildegaard, K., Niaei, A., Hosseini, M., Ebrahimi, S., Sudarsan, S., Angelidaki, I., Borodina, I., 2019. Engineering Oleaginous Yeast as the Host for Fermentative Succinic Acid Production From Glucose. *Front. Bioeng. Biotechnol.* 7. https://doi.org/10.3389/fbioe.2019.00361.

Baker, M., 2012. De novo genome assembly: what every biologist should know. *Nature Methods* 9 (4), 333–337. https://doi.org/10.1038/nmeth.1935.

Beopoulos, A., Nicaud, J.M., Gaillardin, C., 2011. An overview of lipid metabolism in yeasts and its impact on biotechnological processes. *Appl Microbiol Biotechnol* 90 (4), 1193–1206. https://doi.org/10.1007/s00253-011-3212-8.

Blazeck, J., Hill, A., Liu, L., Knight, R., Miller, J., Pan, A., Otoupal, P., Alper, H.S., 2014. Harnessing *Yarrowia lipolytica* lipogenesis to create a platform for lipid and biofuel production. *Nat. Commun* 5 (1). https://doi.org/10.1038/ncomms4131.

Bligh, E.G., Dyer, W.J., 1959. A rapid method of total lipid extraction and purification. *Can J Biochem Physiol* 37 (8), 911–917. https://doi.org/10.1139/y59-099.

Bourque, S.D., Titorenko, V.I., 2009. A quantitative assessment of the yeast lipidome using electrospray ionization mass spectrometry. *J vis Exp* 30. https://doi.org/10.3791/1513.

Breunig, J.S., Hackett, S.R., Rabinowitz, J.D., Kruglyak, L., 2014. Genetic Basis of Metabolome Variation in Yeast. *PLoS Genet* 10 (3), e1004142.

Cao, X., Lv, Y.-B., Chen, J., Imanaka, T., Wei, L.-J., Hua, Q., 2016. Metabolic engineering of oleaginous yeast *Yarrowia lipolytica* for limonene overproduction. *Biotechnol. Biofuels Bioprod.* 9 (1), 214. https://doi.org/10.1186/s13068-016-0626-7.

Cheng, M.-H., Dien, B.S., Lee, D.K., Singh, V., 2019. Sugar production from bioenergy sorghum by using pilot scale continuous hydrothermal pretreatment combined with disk refining. *Bioresour. Technol.* 289, 121663. https://doi.org/10.1016/j.biortech.2019.121663.

Conrad, M., Schothorst, J., Kankipati, H.N., Van Zeebroeck, G., Rubio-Texeira, M., Thevelein, J.M., 2014. Nutrient sensing and signaling in the yeast *Saccharomyces cerevisiae*. *FEMS Microbiol. Rev.* 38 (2), 254–299. https://doi.org/10.1111/1574-6976.12065.

Crabtree, H.G., 1929. Observations on the carbohydrate metabolism of tumours. *Biochem. J.* 23 (3), 536–545. https://doi.org/10.1042/bj0230536.

Demeke, M.M., Foulquié-Moreno, M.R., Dumortier, F., Thevelein, J.M., 2015. Rapid Evolution of Recombinant *Saccharomyces cerevisiae* for Xylose Fermentation through Formation of Extra-chromosomal Circular DNA. *PLoS Genet.* 11 (3), e1005010.

dos Santos, L.V., Carazzolle, M.F., Nagamatsu, S.T., Sampaio, N.M.V., Almeida, L.D., Pirolla, R.A.S., Borelli, G., Corrêa, T.L.R., Argueso, J.L., Pereira, G.A.G., 2016. Unraveling the genetic basis of xylose consumption in engineered *Saccharomyces cerevisiae* strains. *Sci. Rep.* 6 (1), 38676. https://doi.org/10.1038/srep38676.

Friedlander, J., Tsakraklides, V., Kamineni, A., Greenhagen, E.H., Consiglio, A.L., MacEwen, K., Crabtree, D.V., Afshar, J., Nugent, R.L., Hamilton, M.A., Joe Shaw, A., South, C.R., Stephanopoulos, G., Brevnova, E.E., 2016. Engineering of a high lipid producing *Yarrowia lipolytica* strain. *Biotechnol. Biofuels Bioprod.* 9 (1). https://doi.org/10.1186/s13068-016-0492-3.

Fukuda, R., Ohta, A., 2013. Utilization of Hydrophobic Substrate by Yarrowia lipolytica. Microbiology Monographs 111–119. https://doi.org/10.1007/978-3-642-38320-5_5.

Guo, H., Su, S., Madzak, C., Zhou, J., Chen, H., Chen, G., 2016. Applying pathway engineering to enhance production of alpha-ketoglutarate in *Yarrowia lipolytica*. *Appl. Microbiol. Biotechnol.* 100 (23), 9875–9884. https://doi.org/10.1007/s00253-016-7913-x.

Jagtap, S.S., Bedekar, A.A., Singh, V., Jin, Y.-S., Rao, C.V., 2021. Metabolic engineering of the oleaginous yeast *Yarrowia lipolytica* PO1f for production of erythritol from glycerol. *Biotechnol. Biofuels Bioprod.* 14 (1), 188. https://doi.org/10.1186/s13068-021-02039-0.

Jagtap, S.S., Rao, C.V., 2018. Microbial conversion of xylose into useful bioproducts. *Appl. Microbiol. Biotechnol.* 102 (21), 9015–9036. https://doi.org/10.1007/s00253-018-9294-9.

Juanssilfero, A. B., Kahar, P., Amza, R. L., Miyamoto, N., Otsuka, H., Matsumoto, H., Kihira, C., Thontowi, A., Yopi, Ogino, C., Prasetya, B., & Kondo, A. (2018). Selection of oleaginous yeasts capable of high lipid accumulation during challenges from inhibitory chemical compounds. *Biochem. Eng. J.*, **137**, 182–191. https://doi.org/10.1016/j.bej.2018.05.024.

Jumper, J., et al., 2021. Highly accurate protein structure prediction with AlphaFold. Nature 596, 583–589. https://doi.org/10.1038/s41586-021-03819-2.

Kavšček, M., Bhutada, G., Madl, T., Natter, K., 2015. Optimization of lipid production with a genome-scale model of *Yarrowia lipolytica*. *BMC Syst. Biol.* 9 (1), 72. https://doi.org/10.1186/s12918-015-0217-4.

Koh, H.G., Yook, S., Oh, H., Rao, C.V., Jin, Y.-S., 2024. Toward rapid and efficient utilization of nonconventional substrates by nonconventional yeast strains. *Curr. Opin. Biotechnol.* 85, 103059. https://doi.org/10.1016/j.copbio.2023.103059.

Konzock, O., Zaghen, S., Norbeck, J., 2021. Tolerance of *Yarrowia lipolytica* to inhibitors commonly found in lignocellulosic hydrolysates. *BMC Microbiol* 21 (1), 77. https://doi.org/10.1186/s12866-021-02126-0.

Kwak, S., Jin, Y.-S., 2017. Production of fuels and chemicals from xylose by *engineered Saccharomyces cerevisiae*: a review and perspective. *Microb. Cell Fact.* 16 (1), 82. https://doi.org/10.1186/s12934-017-0694-9.

Labun, K., Montague, T.G., Krause, M., Torres Cleuren, Y.N., Tjeldnes, H., Valen, E., 2019. CHOPCHOP v3: expanding the CRISPR web toolbox beyond genome editing. *Nucleic Acids Res.* 47 (W1), W171–W174. https://doi.org/10.1093/nar/gkz365.

Lane, S., Zhang, S., Wei, N., Rao, C., Jin, Y.-S., 2015. Development and physiological characterization of cellobiose-consuming *Yarrowia lipolytica*. *Biotechnol. and Bioeng.* 112 (5), 1012–1022. https://doi.org/10.1002/bit.25499.

Ledesma-Amaro, R., Lazar, Z., Rakicka, M., Guo, Z., Fouchard, F., Coq, A.-M.-C.-L., Nicaud, J.-M., 2016. Metabolic engineering of *Yarrowia lipolytica* to produce chemicals and fuels from xylose. *Metab. Eng.* 38, 115–124. https://doi.org/10.1016/j.ymben.2016.07.001.

Ledesma-Amaro, R., Nicaud, J.-M., 2016. Metabolic Engineering for Expanding the Substrate Range of *Yarrowia lipolytica*. *Trends Biotechnol.* 34 (10), 798–809. https://doi.org/10.1016/j.tibtech.2016.04.010.

Lee, S.-H., Kodaki, T., Park, Y.-C., Seo, J.-H., 2012. Effects of NADH-preferring xylose reductase expression on ethanol production from xylose in xylose-metabolizing recombinant *Saccharomyces cerevisiae*. *J. Biotechnol.* 158 (4), 184–191. https://doi.org/10.1016/j.jbiotec.2011.06.005.

Lee, J.W., Yook, S., Koh, H., Rao, C.V., Jin, Y.-S., 2021. Engineering xylose metabolism in yeasts to produce biofuels and chemicals. *Curr. Opin. Biotechnol.* 67, 15–25. https://doi.org/10.1016/j.copbio.2020.10.012.

Li, H., Alper, H.S., 2016. Enabling xylose utilization in *Yarrowia lipolytica* for lipid production. *Biotechnol. J.* 11 (9), 1230–1240. https://doi.org/10.1002/biot.201600210.

Li, H., Durbin, R., 2009. Fast and accurate short read alignment with Burrows–Wheeler transform. *Bioinform.* 25 (14), 1754–1760. https://doi.org/10.1093/bioinformatics/btp324.

Li, H., Handsaker, B., Wysoker, A., Fennell, T., Ruan, J., Homer, N., Marth, G., Abecasis, G., Durbin, R., Subgroup, G.P.D.P., 2009. The Sequence Alignment/Map format and SAMtools. *Bioinform.* 25 (16), 2078–2079. https://doi.org/10.1093/bioinformatics/btp352.

Malina, C., Yu, R., Björkeroth, J., Kerkhoven, E.J., Nielsen, J., 2021. Adaptations in metabolism and protein translation give rise to the Crabtree effect in yeast. *Proc.natl. Acad. Sci.* 118 (51). https://doi.org/10.1073/pnas.2112836118.

Markham, K.A., Vazquez, S., Alper, H.S., 2018. High-efficiency transformation of *Yarrowia lipolytica* using electroporation. *FEMS Yeast Res.* 18 (7). https://doi.org/10.1093/femsyr/foy081.

McKenna, A., Hanna, M., Banks, E., Sivachenko, A., Cibulskis, K., Kernytsky, A., Garimella, K., Altshuler, D., Gabriel, S., Daly, M., DePristo, M.A., 2010. The Genome Analysis Toolkit: a MapReduce framework for analyzing next-generation DNA sequencing data. *Genome Res.* 20 (9), 1297–1303. https://doi.org/10.1101/gr.107524.110.

Niehus, X., Crutz-Le Coq, A.-M., Sandoval, G., Nicaud, J.-M., Ledesma-Amaro, R., 2018. Engineering *Yarrowia lipolytica* to enhance lipid production from lignocellulosic materials. *Biotechnol. Biofuels* Bioprod. 11 (1), 11. https://doi.org/10.1186/s13068-018-1010-6.

Nijland, J.G., Vos, E., Shin, H.Y., de Waal, P.P., Klaassen, P., Driessen, A.J.M., 2016. Improving pentose fermentation by preventing ubiquitination of hexose transporters in *Saccharomyces cerevisiae*. *Biotechnol. Biofuels Bioprod.* 9 (1), 158. https://doi.org/10.1186/s13068-016-0573-3.

Oh, E.J., Skerker, J.M., Kim, S.R., Wei, N., Turner, T.L., Maurer, M.J., Arkin, A.P., Jin, Y. S., 2016. Gene Amplification on Demand Accelerates Cellobiose Utilization in Engineered *Saccharomyces cerevisiae*. Appl Environ Microbiol. 82 (12), 3631–3639. https://doi.org/10.1128/aem.00410-16.

Papapetridis, I., Verhoeven, M.D., Wiersma, S.J., Goudriaan, M., van Maris, A.J.A., Pronk, J.T., 2018. Laboratory evolution for forced glucose-xylose co-consumption enables identification of mutations that improve mixed-sugar fermentation by xylose-fermenting *Saccharomyces cerevisiae*. *FEMS Yeast Res.* 18 (6). https://doi.org/10.1093/femsyr/foy056.

Pendleton, M., Sebra, R., Pang, A.W.C., Ummat, A., Franzen, O., Rausch, T., Stütz, A.M., Stedman, W., Anantharaman, T., Hastie, A., Dai, H., Fritz, M.-H.-Y., Cao, H., Cohain, A., Deikus, G., Durrett, R.E., Blanchard, S.C., Altman, R., Chin, C.-S., Guo, Y., Paxinos, E.E., Korbel, J.O., Darnell, R.B., McCombie, W.R., Kwok, P.-Y., Mason, C.E., Schadt, E.E., Bashir, A., 2015. Assembly and diploid architecture of an individual human genome via single-molecule technologies. *Nat. Methods* 12 (8), 780–786. https://doi.org/10.1038/nmeth.3454.

Prabhu, A.A., Ledesma-Amaro, R., Lin, C.S.K., Coulon, F., Thakur, V.K., Kumar, V., 2020. Bioproduction of succinic acid from xylose by engineered *Yarrowia lipolytica* without pH control. *Biotechnol. Biofuels Bioprod.* 13 (1), 113. https://doi.org/10.1186/s13068-020-01747-3.

Qiao, K., Wasylenko, T.M., Zhou, K., Xu, P., Stephanopoulos, G., 2017. Lipid production in *Yarrowia lipolytica* is maximized by engineering cytosolic redox metabolism. *Nat. Biotechnol* 35 (2), 173–177. https://doi.org/10.1038/nbt.3763.

Rao, X., Huang, X., Zhou, Z., Lin, X. 2013. An improvement of the 2(-ΔΔCT) method for quantitative real-time polymerase chain reaction data analysis. *Biostat Bioinforma Biomath.*, 3(3), 71-85. PMID: 25558171; PMCID: PMC4280562.

Rodriguez, G.M., Hussain, M.S., Gambill, L., Gao, D., Yaguchi, A., Blenner, M., 2016. Engineering xylose utilization in *Yarrowia lipolytica* by understanding its cryptic xylose pathway. *Biotechnol. Biofuels Bioprod.* 9 (1), 149. https://doi.org/10.1186/s13068-016-0562-6.

Ryu, S., Trinh, C.T., 2018. Understanding Functional Roles of Native Pentose-Specific Transporters for Activating Dormant Pentose Metabolism in *Yarrowia lipolytica*. *Appl Environ Microbiol* 84 (3). https://doi.org/10.1128/aem.02146-17.

Ryu, S., Trinh, C.T., 2021. Methods to Activate and Elucidate Complex Endogenous Sugar Metabolism in *Yarrowia lipolytica*. *Methods and Protocols* 175–189. https://doi.org/10.1007/978-1-0716-1414-3_12.

Ryu, S., Hipp, J., Trinh, C.T., 2015. Activating and Elucidating Metabolism of Complex Sugars in Yarrowia lipolytica. *Appl. Environ. Microbiol.* 82 (4), 1334–1345. https://doi.org/10.1128/aem.03582-15.

Sato, T.K., Tremaine, M., Parreiras, L.S., Hebert, A.S., Myers, K.S., Higbee, A.J., Sardi, M., McIlwain, S.J., Ong, I.M., Breuer, R.J., Avanasi Narasimhan, R., McGee, M.A., Dickinson, Q., La Reau, A., Xie, D., Tian, M., Reed, J.L., Zhang, Y., Coon, J.J., Hittinger, C.T., Gasch, A.P., Landick, R., 2016. Directed Evolution Reveals Unexpected Epistatic Interactions That Alter Metabolic Regulation and Enable Anaerobic Xylose Use by *Saccharomyces cerevisiae*. *PLOS Genet.* 12 (10), e1006372.

Spagnuolo, M., Shabbir Hussain, M., Gambill, L., Blenner, M., 2018. Alternative Substrate Metabolism in *Yarrowia lipolytica*. *Front. Microbiol.* 9, 1077. https://doi.org/10.3389/fmicb.2018.01077.

Spagnuolo, M., Yaguchi, A., Blenner, M., 2019. Oleaginous yeast for biofuel and oleochemical production. *Curr. Opin. Biotechnol.* 57, 73–81. https://doi.org/10.1016/j.copbio.2019.02.011.

Sun, L., Lee, J.W., Yook, S., Lane, S., Sun, Z., Kim, S.R., Jin, Y.-S., 2021. Complete and efficient conversion of plant cell wall hemicellulose into high-value bioproducts by engineered yeast. *Nat. Commun* 12 (1), 4975. https://doi.org/10.1038/s41467-021-25241-y.

Tai, M., Stephanopoulos, G., 2013. Engineering the push and pull of lipid biosynthesis in oleaginous yeast *Yarrowia lipolytica* for biofuel production. *Metab. Eng.* 15, 1–9. https://doi.org/10.1016/j.ymben.2012.08.007.

Tanaka, K., Lin, B.K., Wood, D.R., Tamanoi, F., 1991. IRA2, an upstream negative regulator of RAS in yeast, is a RAS GTPase-activating protein. *Proc Natl Acad Sci U S A* 88 (2), 468–472. https://doi.org/10.1073/pnas.88.2.468.

Van, G., & O'connor, B. D. (2020). Genomics in the cloud : using Docker, GATK, and WDL in Terra. O'reilly Media.

Yook, S.D., Kim, J., Woo, H.M., Um, Y., Lee, S.-M., 2019. Efficient lipid extraction from the oleaginous yeast *Yarrowia lipolytica* using switchable solvents. *Renew. Energy* 132, 61–67. https://doi.org/10.1016/j.renene.2018.07.12.

Yook, S.D., Kim, J., Gong, G., Ko, J.K., Um, Y., Han, S.O., Lee, S.-M., 2020. High-yield lipid production from lignocellulosic biomass using engineered xylose-utilizing *Yarrowia lipolytica*. *GCB Bioenergy* 12 (9), 670–679. https://doi.org/10.1111/gcbb.12699.

Yuzbasheva, E.Y., Agrimi, G., Yuzbashev, T.V., Scarcia, P., Vinogradova, E.B., Palmieri, L., Shutov, A.V., Kosikhina, I.M., Palmieri, F., Sineoky, S.P., 2019. The mitochondrial citrate carrier in *Yarrowia lipolytica*: Its identification, characterization and functional significance for the production of citric acid. *Metab. Eng.* 54, 264–274. https://doi.org/10.1016/j.ymben.2019.05.002.

Zheng, N., Shabek, N., 2017. Ubiquitin Ligases: Structure, Function, and Regulation. *Annu. Rev. Biochem.* 86 (1), 129–157. https://doi.org/10.1146/annurev-biochem-060815-014922.